NASA TECHNICAL NOTE

NASA TN D-7698

NASA TN D-7698

GRAPHITE-POLYIMIDE COMPOSITE FOR APPLICATION TO AIRCRAFT ENGINES

by Morgan P. Hanson and Christos C. Chamis

Lewis Research Center
Cleveland, Ohio 44135

NATIONAL AERONAUTICS AND SPACE ADMINISTRATION • WASHINGTON, D. C. • JUNE 1974

1. Report No.	2. Government Accession No.	3. Recipient's Catalog No.
NASA TN D-7698		

4. Title and Subtitle	5. Report Date
GRAPHITE-POLYIMIDE COMPOSITE FOR APPLICATION TO AIRCRAFT ENGINES	JUNE 1974
	6. Performing Organization Code

7. Author(s)	8. Performing Organization Report No.
Morgan P. Hanson and Christos C. Chamis	E-7700
	10. Work Unit No. 501-21

9. Performing Organization Name and Address	11. Contract or Grant No.
Lewis Research Center National Aeronautics and Space Administration Cleveland, Ohio 44135	

12. Sponsoring Agency Name and Address	13. Type of Report and Period Covered
National Aeronautics and Space Administration Washington, D.C. 20546	Technical Note
	14. Sponsoring Agency Code

15. Supplementary Notes

16. Abstract

A combined experimental and theoretical investigation was performed in order to (1) demonstrate that high quality angleplied laminates can be made from HT-S/PMR-PI (PMR in situ polymerization of monomeric reactants), (2) characterize the PMR-PI material and to determine the HT-S unidirectional composite properties required for composite micro and macromechanics and laminate analyses, and (3) select HT-S/PMR-PI laminate configurations to meet the general design requirements for high-tip-speed compressor blades. The results of the investigation showed that HT-S/PMR laminate configurations can be fabricated which satisfy the high-tip-speed compressor blade design requirements when operating within the temperature capability of the polyimide matrix.

17. Key Words (Suggested by Author(s))	18. Distribution Statement
Compressor blades; High-tip-speed; Elevated temperature; Fiber composites; Polyimide matrix; Polyimide resin; Graphite fibers; Testing; Composite characterization; Composite mechanics; Design requirements	Unclassified - unlimited Category 32

19. Security Classif. (of this report)	20. Security Classif. (of this page)	21. No. of Pages	22. Price*
Unclassified	Unclassified	27	$3.25

* For sale by the National Technical Information Service, Springfield, Virginia 22151

GRAPHITE-POLYIMIDE COMPOSITE FOR APPLICATION TO AIRCRAFT ENGINES

by Morgan P. Hanson and Christos C. Chamis

Lewis Research Center

SUMMARY

A combined experimental and theoretical investigation was performed to (1) demonstrate that high quality angleplied laminates can be made from HT-S/PMR-PI (PMR - in situ polymerization of monomeric reactants), (2) characterize the PMR-PI material and determine the HT-S unidirectional composite properties required for composite micromechanics, macromechanics, and laminate analyses, and (3) select HT-S/PMR laminate configurations to meet the general design requirements for high-tip-speed compressor blades.

Test specimens were made from the PMR neat resin and from HT-S/PMR-PI unidirectional composites. HT-S/PMR-PI laminates were made with ply configurations simulating those considered for high-tip-speed compressor blade applications. The coefficients of thermal expansion and mechanical properties of the PMR-PI resin and HT-S fiber composites were evaluated. The simulated blade laminates were tested to fracture in tension and flexure. Laminate analysis and composite macromechanics and micromechanics were used to calculate the stresses in the plies due to lamination residual stresses, applied load to fracture, and a combination of the two. Available combined-stress - strength criteria were used to determine the margin of safety or failure of the plies under applied load. The properties of blade-type laminates were compared with the general design requirements for ultra-high-tip-speed composite compressor blades.

The results of the investigation showed that HT-S/PMR laminate configurations can be fabricated to satisfy the high-tip-speed compressor blade design requirements when operating within the temperature capability of the polyimide matrix. The fabrication process (in situ polymerization) enhances the in situ intralaminar shear strength and the ply transverse strength. The tensile strength notch sensitivity of unidirectional composites with high short-beam-shear strength can be alleviated by orienting some of the plies at relatively low angles (less than $\pm 10^{\circ}$) to the load direction. The presence of lamination residual stresses decreases the fracture strength of angleplied laminates. A combined experimental and theoretical investigation is the most direct approach to obtain an assessment of the applications of new advanced composites to specific designs.

INTRODUCTION

Advanced aircraft engines designed with high-speed axial-flow compressor stages will require high performance composites with high strength retention at high temperatures. Preliminary investigation of HT-S/PMR-PI composites (ref. 1) showed that they can meet the requirements for advanced engine compressors that operate within the temperature capability of the PMR-PI resin.

To establish the suitability of HT-S/PMR-PI composites for advanced aircraft engine applications a combined experimental and theoretical investigation was performed. This investigation was performed in the following manner: Test specimens were made from the PMR-PI neat resin and from HT-S/PMR-PI unidirectional composites. The HT-S/PMR-PI laminates were made with ply configurations simulating those considered for high-tip-speed compressor blade applications. The coefficients of thermal expansion and mechanical properties; that is, Izod impact, tensile and flexural strengths, and stiffness of the PMR-PI resin and HT-S fiber composites were evaluated and used in the laminate analysis and composite macromechanics and micromechanics. The simulated blade laminates were tested to fracture in tension and flexure. Laminate analysis and composite macromechanics and micromechanics were used to calculate the stresses in the plies due to lamination residual stresses, applied load to fracture, and the combination of the two. Available combined-stress - strength criteria were used to determine the margin of safety or failure of the plies under applied load. The properties of blade-type laminates were compared with the general design requirements for ultra-high-tip-speed composite compressor blades.

EXPERIMENTAL PROGRAM

The experimental program was undertaken to determine mechanical properties as related to the application of graphite-fiber/polyimide resins to advanced aircraft engine applications. The results are used to verify quantitatively the theoretical considerations and concepts described in the Theoretical Investigation section. Materials evaluated were of the neat resin and graphite/resin composites in various ply orientations.

MATERIALS AND SPECIMEN FABRICATION

Neat Resin

The monomer solution was formulated from the monomeric reactants (1) 4, 4'-methylenedianiline (MDA) and (2) a monomethylester of 5-norbornene-2, 3-dicarboxylic

acid (NE) and a dimethylester of 3, 3', 4, 4'-benzophenonetetracarboxylic acid (BTDE) with methyl alcohol as the solvent. The solution was prepared according to the procedure reported in reference 1 (sample 1).

Molded neat resin was prepared by drying the solution and grinding it to a powder. The powder was then imidized at 204° C (400° F) for 2 hours. The powder was placed in a cold mold and compacted under 345 newtons per square centimeter (500 psi) pressure. With the pressure released, the mold was heated to 274° C (525° F). At this point a mold pressure of 345 newtons per square centimeter (500 psi) was applied and the temperature increased to 316° C (600° F). After 1 hour the resin was cured.

Laminate Fabrication

The HT-S fiber was drum wound and impregnated with the PMR-PI resin. The resin was in a alcohol solvent solution having a solids content of 50 percent by weight. A predetermined quantity of resin solution was applied to the fiber so that the final cured laminate would have a fiber volume ratio of 0.55. Heat lamps were used to reduce the solvent content to approximately 10 percent before removing the prepreg from the drum. The prepared prepreg had a thickness of 0.20 millimeter (0.008 in.). Unidirectional and various angleplied laminates were cut to mold size, 7.62 by 25.4 centimeters (3 by 10 in.), to fabricate the laminates listed in table II.

The plies were stacked between porous TFE-coated glass-cloth, placed in a mold sized tray and compacted with a 4.53-kilogram (10-lb) weight. The preform was imidized in an air-circulating oven at 204° C (400° F) for 2 hours. The Teflon-coated glass-cloth was removed and the preform was placed between aluminum caul plates and placed in the preheated 204° C (400° F) mold. The cure cycle is shown graphically in figure 1. Since the laminate exhibits a thermoplastic behavior in the as-cured condition, all laminates were post-cured as noted in figure 1.

Specimen Fabrication

Neat-resin tensile specimens were machined from 3.2 millimeter (0.125-in.) thick material in accordance with ASTM standard method D638-type 1. Compression specimens were machined from 12.7- by 38-millimeters (0.5- by 1.5-in.) coupons to provide a 6.3- by 19.1-millimeter (0.25- by 0.75-in.) test section.

Longitudinal tensile specimens (1.27 by 25.4 cm (0.5 by 10 in.)) of the HT-S/PMR-PI were machined from the 7.62 by 25.4 centimeter (3 by 10 in.) laminates with the 0° fiber plies in the 25.4-centimeter (10-in.) direction. The specimens had parallel sides

with 6.3 centimeter (2.5-in.) long reinforcing tabs adhesively bonded to the ends. Transverse tensile specimens were machined from 1.27 by 7.6 centimeter (0.5 by 3 in.) coupons. The test section of the finished specimen was 6.3 by 38 millimeter (0.25 by 1.5 in.) The 6.3-millimeter (0.25-in.) reinforced holes on the ends were provided for load application.

Miniature Izod specimens (5.1 mm (0.20 in.) thick) were machined from 0° ply composites. The finished specimen dimensions were 5.1 by 5.1 by 37.6 millimeters (0.2 by 0.2 by 1.48 in.).

TEST APPARATUS AND PROCEDURE

Tensile, flexure, and interlaminar shear tests were performed in a universal testing machine with a selected constant-speed crosshead.

Tensile tests of the neat resin were performed in accordance with ASTM method D638 at a crosshead speed of 2.5 millimeters per minute (0.1 in./min). The various composite tensile specimens were tested at 1.3 millimeters per minute (0.05 in./min). Strain to fracture was measured with a clamp-on extensometer.

The flexure specimens were tested using the ASTM standard method D790-71-Method I. Tests were made on a three-point loading fixture having a span of 5.1 centimeters (2.0 in.). The short-beam interlaminar shear specimens were tested using a three-point loading fixture having a span to thickness ratio of 5:1.

Izod specimens were tested in a modified Bell Telephone Laboratory pendulum impact machine. The striking velocity of the pendulum was 345 centimeters per second (136 in./sec). The Izod specimens were struck at their free end, 22 millimeters (0.87 in.) from the edge of the cantilever grip.

The coefficients of thermal expansion were determined for the neat resin and longitudinal and transverse uniaxial composite material. Coupons of resin and composite were heated from 38° to 316° C (75° to 600° F) and the change in dimension was measured. The change in temperature was measured using imbedded thermocouples.

EXPERIMENTAL RESULTS AND DISCUSSION

The results obtained from the experimental investigation of neat resin and composite material consist of stress-strain diagrams, and mechanical and physical properties.

The stress-strain diagram of the PMR-PI neat resin is shown in figure 2. The relation is essentially linear to fracture. The modulus of the neat resin 0.33×10^{6} newtons per square centimeter (0.47×10^{3} ksi) is a typical value of PI resin systems. The

stress-strain diagrams of the various angleplied composites are shown in figure 3. It can be seen that the modulus of 15.0×10^6 newtons per square centimeter (21.7×10^3 ksi) is typical of uniaxial HT-S composites with 55-percent fiber volume. It is also noted that the two composites with 10° plies have moduli similar to the uniaxial composite (14.6×10^6 and 13.1×10^6 N/cm^2 or 21.1×10^3 and 19.0×10^3 ksi). The $\pm40^\circ$ and 0° ply laminate shows a lower modulus than would be expected with the predominance of 0° plies. Possible causes for this behavior will be discussed in the section, Theoretical Program.

Tables I and II summarize the strength properties of the neat resin and composite materials. The data are an average of three or more tests for the particular property. Although most of the HT-S/PMR-PI composite strength properties are comparable with those reported of other HT-S/resins composite materials, the tensile strength of the PMR-PI neat resin may be lower than the actual value due to the inherent limitation of the molding process of the resin. Also the low compressive strength of the composite material may not be a realistic value because of the inherent limitations of the test method.

THEORETICAL PROGRAM

The theoretical program consisted of two parts: (1) the selection of the correlation coefficients required in the computer code (ref. 2) to carry out the composite micromechanics and macromechanics and (2) the laminate analyses of the various laminates tested. These parts are essential in assessing both the potential of the HT-S/PMR-PI composite for high-tip-speed compressor blade applications and the in situ PMR-PI matrix performance. The notation used herein is defined when it first appears and, again, in the appendix for convenience.

SELECTION OF CORRELATION COEFFICIENTS

Two sets of correlation coefficients are required in the computer code (ref. 2): the first, to predict unidirectional composite thermal and elastic properties from corresponding constituent properties and, the second, to predict unidirectional composite strength properties.

Correlation Coefficients for Thermal and Elastic Properties

The constituent material properties required to predict composite properties from constituent properties using composite micromechanics are summarized in table III.

The correlation coefficients for thermal and elastic properties were the same as those for type II-fiber/resin matrix composites. (See ref. 2, table XI.) This is consistent with previous experience (ref. 3) when it was found that the correlation coefficients for elastic and thermal properties appear insensitive to the types of fiber-resin.

Correlation Coefficients for Unidirection Composite Strengths

Five unidirectional composite strengths are required to characterize a unidirectional composite from the strength viewpoint. These strengths are longitudinal tension ($S_{\ell 11T}$), longitudinal compression ($S_{\ell 11C}$), transverse tension ($S_{\ell 22T}$), transverse compression ($S_{\ell 22C}$) and intralaminar shear ($S_{\ell 12S}$). These strengths can be predicted from corresponding constituent properties using composite micromechanics. The main advantage for relating composite strength to constituent properties is that the micromechanics in the computer code provides for in situ ply strength. The constituent material properties required for predicting these strengths by means of micromechanics are summarized in table IV. The values of the correlation coefficients used in the computer code are listed in table V.

Two important points can be made from the values of the strength correlation coefficients in table V:

(1) The value of β_{fT} is 0.94, which is close to unity. This indicates a relatively high matrix efficiency in translating fiber strength to composite.

(2) The values of the strength correlation coefficients β_{22T}, β_{22C}, and β_{12S} are unity or higher. Such values indicate that the in situ PMR-PI matrix strength is equal to or better than its bulk state strength. Point (2) attains additional importance in that the values of these strength correlation coefficients are about 0.5 for other fiber-resin composites.

The important conclusion from the preceding discussion is that in situ polymerization appears to enhance the fiber-matrix interfacial bond and the in situ matrix strength, which results in improved intralaminar shear and transverse tensile strengths for the unidirectional composite.

Measured and predicted unidirectional composite properties are summarized in table VI for comparison. Some items in table VI need additional explanation.

(1) No measured data are available for the thermal heat conductivities for the composite or the PMR-PI matrix. The predicted values shown in table VI are based on the estimated matrix data shown in table III. They are included here merely as indications. Also, no measured data are available for composite shear modulus or Poisson's ratio.

(2) The limiting value of the transverse compressive stress ($S_{\ell 22C}$) was taken to be about 80 percent of the corresponding fracture stress. This was done because, in gen-

eral, transverse compression - stress-strain curves exhibit excessive nonlinearities beyond the 80-percent fracture stress value.

(3) The intralaminar shear strength ($S_{\ell 12S}$) was taken to be about 50 percent of the short-beam-shear fracture-stress value. This was done for two reasons: (a) Results of angleplied laminate analyses has indicated that, in predominantly shear-failed laminates, the intralaminar shear stress was about one-half of the short-beam-shear fracture stress; and (b) S-glass fiber/resin unidirectional thin tubes subjected to torsion fracture at a shear stress of about 50 to 60-percent of the corresponding short-beam-shear fracture stress.

An examination of the measured and predicted property values in table VI shows that the selected correlation coefficients yield predicted values that are in good agreement with the measured data.

The preceding discussion leads to the following tentative recommendation: The intralaminar shear strength should be taken to be one-half of the short-beam-shear (interlaminar) fracture stress.

LAMINATE ANALYSIS OF ANGLEPLIED LAMINATES

The computer code (ref. 2) was used to analyze the laminates. The analysis yielded the following laminate properties: (1) thermal and elastic constants, (2) plate bending stiffnesses, and (3) ply stresses and margin of safety due to cure temperature, axial fracture load, bending fracture moment, and combinations of these. This type of information can be used to:

(1) Assess the application of linear laminate theory to HT-S/PMR-PI composites.

(2) Establish whether any or all of the laminates meet the general design requirements of the high-tip-speed compressor blade.

Laminate Elastic Constants and Thermal Coefficients of Expansion

The elastic constant and thermal coefficients of expansion of the laminate were calculated using the unidirectional composite properties in table VI. The results are summarized in table VII. The information in table VII can be used to select ply arrangements for the blade core and the blade shell. Based on composite blade general design requirements (to be described later), the laminates 6[0], 4[±10, ∓10], and 8[0, +10, 0, -10, -10, 0, +10, 0] are suitable for the blade core, and the laminate 4[±40, ∓40] is suitable for the blade shell. The laminate 13[±40, 9(0), ∓40] is representative of the blade at its maximum thickness point. This laminate has a negative thermal coefficient

of expansion along the x-direction (α_{cxx}). This is an advantage because it counteracts the radial growth of the blade due to centrifugal loads.

Three other points should be mentioned about table VII:

(1) The laminate properties in table VII are based on 0.55 fiber volume ratio. This value was selected because laminates from HT-S/PMR-PI under well controlled fabrication conditions are expected to have a fiber volume ratio of about 0.55.

(2) Some laminates tested in this investigation could have had fiber volume ratios different than 0.55.

(3) The predicted laminate moduli (E_{cxxx}) in table VII differ from the measured values in table II. This difference could be caused by any one or by a combination of the following factors: difference in fiber volume ratio, deviations in the ply orientation angle, deviations between actual and predicted shear modulus, bending due to testing load eccentricity and ply relative rotation.

The important point of this discussion is that HT-S/PMR-PI laminate configurations can be selected that appear to be suitable for compressor blade application from the thermal and elastic constants considerations. It should also be noted that the 8[0, +10, 0, -10, -10, 0, +10, 0] laminate has greater tensile strength then the 6(0) laminate (table II). This indicates that the notch sensitivity of unidirectional composite with high interlaminar shear strength can be alleviated by orienting some of the plies at relatively low angles (10^{o} or less) to the load direction.

Laminate Bending Stiffnesses

The laminate bending stiffnesses are a good measure on how a fiber-composite compressor blade will perform when subjected to combined loadings and how they will resist vibrations and flutter. The laminate bending stiffness of interest herein are the coefficients in the matrix equation:

$$\begin{Bmatrix} M_{cxx} \\ M_{cyy} \\ M_{cxy} \end{Bmatrix} = \begin{bmatrix} D_{c11} & D_{c12} & D_{c13} \\ D_{c21} & D_{c22} & D_{c23} \\ D_{c31} & D_{c32} & D_{c33} \end{bmatrix} \begin{Bmatrix} \kappa_{cxx} \\ \kappa_{cyy} \\ \kappa_{cxy} \end{Bmatrix} \tag{1}$$

where M is moment, D is bending stiffness, and κ is curvature. The subscript c denotes composite property. The subscripts xx, yy, and xy represent structural axes directions. The subscripts 11, 22, etc., represent positions in the array. The D array is symmetric; that is, $D_{c12} = D_{c21}$, $D_{c31} = D_{c13}$, and $D_{c32} = D_{c23}$. The physi-

cal meaning of the various D's is as follows: D_{c11} is the bending stiffness along the x-direction, D_{c22} is the bending stiffness along the y-direction, D_{c33} is the torsional stiffness, D_{c12} is the bending resistance along the x-direction due to a moment in the y-direction, D_{c13} is the bending resistance along the x-direction due to a torsional moment, and D_{c23} is the bending resistance along the y-direction due to a torsional moment. The symmetric coefficients D_{c21}, D_{c31}, and D_{c32} have analogous physical meaning.

In fiber composite compressor blade design, the bending stiffnesses are used to assess blade response as follows:

D_{c11} controls the tip deflection and the uncoupled span-wise vibration bending modes.

D_{c22} controls the uncambering and the uncoupled chord-wise vibration bending modes.

D_{c33} controls the untwist and the uncoupled twisting vibration modes.

The coefficients D_{c12}, D_{c13}, and D_{c23} control the coupled responses indicated by their subscripts.

In selecting laminate configurations for compressor blades, the procedure usually is as follows:

(1) Select a laminate with a high value for D_{c11}.

(2) Adjust the ply orientations until the values for D_{c22} and D_{c33} are within a priori estimated ratios of D_{c11}. The a priori estimated ratios depend on the span-to-chord ratio of the blade and could vary between 10 and 100 percent at the maximum blade thickness.

(3) Retain ply orientations which yield relatively low values for the coupled coefficients D_{c13} and D_{c23}.

It was mentioned in the last section that the laminate $13[\pm 40, 9(0), \mp 40]$ was a good candidate for the high-tip-speed compressor blade. The bending stiffnesses of this laminate are summarized in table VIII. Note that the values of D_{c13} and D_{c23} are relatively small compared with D_{c11}. Note also that the values of D_{c22} and D_{c33} are about 25 to 30 percent of D_{c11}. These values are consistant with the guidelines for selecting laminate configurations for compressor blading.

The laminate bending modulus can be obtained from the bending stiffness by means of the following equation:

$$E_{cxx} = 12D_{cxx}\frac{(1 - \nu_{cxy}\nu_{cyx})}{t_c^3} \tag{2}$$

where

$$D_{cxx} = D_{c11}$$

$$\nu_{cxy} = \frac{D_{c12}}{D_{c22}} \tag{3}$$

$$\nu_{cyx} = \frac{D_{c12}}{D_{c11}}$$

and t_c is the laminate thickness. Using values for D_{c11}, D_{c12}, and D_{c22} from table VIII and $t_c = 0.27$ centimeter (0.106 in.) in the equation for E_{cxx} yields 6.69×10^6 newtons per square meter (9.7×10^3 ksi). The corresponding measured value from table II is 6.41×10^6 newtons per square centimeter (9.3×10^3 ksi), which is in good agreement with the predicted value.

Bending moduli were also computed for the other laminates tested. The predicted values for these laminates were about the same as the values for the E_{cxx} in table VII. These values differ from the measured data. This difference could be caused by the factors causing the difference in the tensile moduli as mentioned in the last section. Additional factors that could cause the difference between measured and predicted bending moduli are relatively small numbers of plies (less than 10), which could violate the linear laminate theory assumptions, strong coupling between bending and twisting, and local indentation of the specimen at the support and loading points. Two conclusions follow from the previous discussion:

(1) Laminate configurations for preliminary blade designs can be readily selected by laminate analysis when a priori estimates on the bending stiffnesses are available.

(2) For angleplied laminates with relatively large numbers of plies (greater than 10), measured and predicted values of the bending modulus are in good agreement.

Conclusion (2) is significant because it proves that linear laminate theory is applicable to angleplied laminates from HT-S/PMR-PI composites. It also provides confidence in the predictions of blade deflections and frequencies by linear laminate theory.

Ply Stresses

The stresses and the margin of safety in the plies of the laminates investigated were determined using linear laminate theory. The linear laminate theory used is embedded in the computer code (ref. 2). The application of linear laminate theory for these calculations is valid because the laminates exhibit linear stress-strain curves to fracture (fig. 3).

Ply stresses and margins of safety were determined due to:

(1) Cure temperature (residual stresses)

(2) Axial fracture load with no residual stresses

(3) Bending fracture moment with no residual stresses

(4) Axial fracture load with residual stresses

(5) Bending fracture moment with residual stresses.

The inputs for these calculations consisted of:

(1) Constituent limit properties (table IV)

(2) Strength correlation coefficients (table V)

(3) Ply elastic and thermal properties (table VI)

(4) Cure temperature difference, which equals cure temperature minus room temperature (295° C (530° F))

(5) Specimen axial fracture load

(6) Specimen bending fracture moment

(7) Laminate configuration.

The margin of safety was determined using a modified distortion energy principle for a combined-stress - failure criterion (ref. 3). The purpose of these calculations was to:

(1) Assess the applicability of linear laminate theory to failure analysis of HT-S/PMR-PI angleplied laminates

(2) Obtain an indirect assessment of the in situ ply strength

(3) Determine whether the residual stresses would cause transply cracks.

The underlying consideration on the ply stress analysis calculations was the following: Fracture axial loads or bending moments, either singly or in combination with residual stresses, should produce ply combined-stress states with negative values for the margin of safety. This procedure is used to design structural components from angleplied laminates to satisfy strength requirements.

The ply stress calculation results are summarized in table IX for the 6[0] laminate, table X for the 4[±10, ∓10] laminate, table XI for the 8[0, +10, 0, -10, -10, 0, +10, 0] laminate, and in table XII for the 13[±40, 9(0), ∓40] laminate. In these tables the type of loading and the ply at which stresses were calculated are listed in the columns headed by "Thermal Load due to cure." The stresses due to mechanical loads without residual stress are listed in the columns headed by "Mechanical load." The combined stresses due to mechanical and thermal loads are listed in the columns headed by "Combined loads."

The notation in these tables is as follows: $\sigma_{\ell 11}$ denotes longitudinal ply stress (along the fiber direction), $\sigma_{\ell 22}$ denotes transverse ply stress, $\sigma_{\ell 12}$ denotes the in-plane (intralaminar) shear stress. The margin of safety was computed by the modified distortion energy principle.

The three important points from the results shown in tables IX to XII are:

(1) The margin of safety for the residual stresses is positive for all the laminates. Thus, residual stresses do not cause transply cracks in the laminate configurations investigated.

(2) The margin of safety is negative, or nearly so, for one or more plies in each of the laminates when subjected to mechanical load only. This indicates that at fracture load or bending moment one or more of the plies failed.

(3) The margin of safety is negative for one or more plies in each of the laminates for the combined load case. The values of the margins of safety for this case are more negative than for the mechanical-load-only case. This indicated a possible enhancement in the in situ ply strengths as was previously mentioned.

Also, the presence of lamination residual stresses tends to decrease the load carrying capacity of the laminates. The previous discussion leads to the following important conclusions with regard to HT-S/PMR-PI laminates representative for compressor blade applications:

(1) Laminate failure as predicted by linear laminate theory is conservative.

(2) There appears to be significant transverse and intralaminar shear strength enhancement in the in situ plies.

(3) The lamination residual stresses do not cause transply cracks.

These conclusions become even more significant because linear theory was used and the laminates investigated exhibited linear stress-strain curves to fracture.

An additional important conclusion follows from the ply stresses of the laminate $13[\pm 40, 9(0), \mp 40]$ in table XII: the zero plies have positive margins of safety; therefore, the zero plies were not used to their maximum efficiency. One way to correct this situation, is to intersperse a few 0° plies with the shell plies.

APPLICATION OF HT-S/PMR-PI COMPOSITES TO ADVANCED AIRCRAFT ENGINES

A two-phase procedure is used herein to determine the suitability of HT-S/PMR-PI composites for advanced aircraft engine application. In the first phase we examine the general design requirements of the high-tip-speed compressor blade. In the second phase we compare the laminate properties obtained previously with the blade general design requirements. The criterion for establishing suitability is that one or more of the laminates investigated meet the blade general design requirements.

General Design Requirements for an Ultra High-Tip-Speed Compressor Composite Blade

The general design requirements for a high-tip-speed (671 m/sec (2200 ft/sec)) compressor blade from fiber composite materials are:

(1) The core laminate configuration should have a tensile modulus of 12.4×10^6 newtons per square centimeter (18×10^3 ksi) or greater.

(2) The shell laminate configuration should have a shear modulus of 2.76×10^6 newtons per square centimeter (4×10^3 ksi) or greater.

(3) The core laminate configuration should have a tensile strength of 62.1×10^3 newtons per square centimeter (90 ksi) or greater at room temperature.

(4) The blade laminate configuration should be free of transply cracks due to cure temperature.

(5) The blade laminate configuration should retain its structural integrity in the temperature range -51° to 260° C (-60° to 500° F).

(6) The unidirectional laminate should retain 70 percent or more of its longitudinal tensile properties at about 288° C (550° F) for long exposures, and it should retain 50 percent or greater of its other unidirectional properties.

(7) The chordwise and torsional stiffnesses of the blade laminate configuration should be about 25 to 30 percent of the spanwise bending stiffness.

(8) The blade laminate configuration should have good resistance to cyclic load.

(9) The unidirectional laminate should have longitudinal Izod impact energy resistance of 113.0 centimeter-newtons (10 in.-lb) or greater.

Comparison of Design Requirements with the Properties of the HT-S/PMR-PI Angleplied Laminates

Design requirements 1, 2, and 3. - Comparison of the measured or predicted stiffness and strength properties of the laminates 6[0], 4[±10, ∓10], 8[0, +10, 0, -10, -10, 0, +10, 0] indicate that they meet the design requirements for the core. The predicted shear modulus for the laminate 4[±40, ∓40] meets the design requirements for the shell.

Design requirements 4 and 7. - The blade laminate configuration 13[±40, 9(0), ∓40] meets the residual stress requirements and the bending stiffness requirement. It is noted that the average tensile strength of this laminate meets the design requirements of the core. Also, the modulus and tensile strength of this laminate are comparable with titanium alloys, which are commonly used for compressor blades. This is significant since the titanium is three times heavier.

Design requirements 5 and 6. - The high-temperature-strength stiffness retention of HT-S/PMR-PI unidirectional composites was investigated in reference 1. It was found that these composites retain about 70 percent of their room-temperature-flex stiffness strength at 316° C (600° F) for long exposures. The corresponding interlaminar shear strength retention was 50 percent or greater.

Design requirement 8. - Graphite fiber-nonmetallic matrix composites have good cyclic load resistance. Unidirectional composites cyclicly loaded at 80 percent of their static strength exceed 10^6 cycles in general (ref. 4).

Design requirement 9. - The measured longitudinal Izod impact resistance for an HT-S/PMR-PI unidirectional laminate is 171.8 centimeter-newtons (15.2 in.-lb), which is 1.5 times greater than the design requirement (see table II).

This comparative discussion leads to the following conclusion. HT-S/PMR-PI laminates can be selected which meet all the general design requirements for a high-tip-speed composite compressor blade. Of the laminates investigated, the laminate 8[0, +10, 0, -10, -10, 0, +10, 0] is the best configuration for the blade core. The laminate configuration of $\pm 40^{\circ}$ interspersed with a few 0° plies appears to be a good candidate for the shell.

CONCLUDING REMARKS

The HT-S/PMR-PI laminates can be fabricated to meet all the general design requirements for a high-tip-speed composite compressor blade operating within the temperature capability of the PMR-PI resin.

Of the laminates investigated for the 671-meter-per-second (2200-ft/sec) blade application, the laminate 8[0, +10, 0, -10, -10, 0, +10, 0] is the best configuration for the blade core and $\pm 40^{\circ}$ interspersed with a few 0°-plies for the shell.

A combined experimental and theoretical investigation is the most direct approach to obtain a broad assessment of the application of new advanced composites to specific designs.

Laminate failure as predicted by linear laminate theory is conservative. There appears to be a significant transverse and intralaminar shear strength enhancement in the in situ plies. The lamination residual stresses do not cause transverse ply cracks in representative laminate configurations for compressor blade applications.

The in situ polymerization process enhances the fiber-matrix interfacial bond and the in situ matrix strength resulting in improved unidirectional composite transverse tensile and intralaminar shear strengths.

Lewis Research Center,
National Aeronautics and Space Administration,
Cleveland, Ohio, March 12, 1974,
501-21.

APPENDIX - SYMBOLS

a_1, a_2 unidirectional composite strength correlation coefficients (table V)

D bending (flexural) stiffness, subscripts define type (eq. (1))

E normal modulus, subscripts define type (table VI)

G shear modulus, subscripts, define type (table VI)

K thermal heat conductivities, subscripts define type (tables III and VI)

K_{l12} coefficient for combined stress

M bending moment, subscripts define direction (eq. (1))

S unidirectional composite strength, subscripts define type and sense (table VI)

t_c laminate (composite) thickness

α thermal coefficients of expansion subscripts define type and direction (tables III, VI, and VII)

β correlation coefficients defined in table V

ϵ strains, subscripts define type and direction

κ curvatures, subscripts define type and direction

ν Poisson's ratio, subscripts define type and direction (tables III, VI, and VII)

ρ density, subscripts define type (table III)

σ stress, subscripts define type and direction

Subscripts:

C compression property

c composite property

f fiber property

l unidirectional composite (ply) property

m matrix property

p limit value

S shear property

T tensile property

x, y, z structural axes coordinate directions

1, 2, 3 type or material axes coordinate directions

REFERENCES

1. Delvigs, Peter; Serafini, Tito T.; and Lightsey, George R.: Addition-Type Polyimides from Solutions of Monomeric Reactants. NASA TN D-6877, 1972.

2. Chamis, Christos C.: Computer Code for the Analysis of Multilayered Fiber Composites - Users Manual. NASA TN D-7013, 1971.

3. Chamis, Christos C.: Failure Criteria for Filamentary Composites. NASA TN D-5367, 1969.

4. Hanson, Morgan P.: Tensile and Cyclic Fatigue Properties of Graphite Filament-Wound Pressure Vessels at Ambient and Cryogenic Temperatures. NASA TN D-5354, 1969.

TABLE I. - ROOM TEMPERATURE PROPERTIES OF

[a]PMR-PI NEAT RESIN

Tensile strength, N/cm^2, psi	5580; 8100
Tensile modulus, N/cm^2; psi	0.32×10^6; 0.47×10^6
Compressive yield strength, N/cm^2; psi	11 400; 16 500
Compressive strength, N/cm^2; psi	18 700; 27 200
Thermal coefficient of expansion, cm/cm/°C; in./in./°F	50.4×10^{-6}; 28.0×10^{-6}

[a]NE/MDA/BTDE (ref. 1); formulated molecular weight, 1500.

TABLE II. - PROPERTIES OF HT-S/PMR-PI COMPOSITES

[Fiber volume, 55 vol %; tested along 0° ply direction.]

Laminate	Tensile strength		Tensile modulus		Compressive strength		Flexural strength	
	N/cm^2	psi	N/cm^2	psi	N/cm^2	psi	N/cm^2	psi
6[0]	124 000	180 000	15.0×10^6	21.7×10^6	93 000	135 000	141 900	206 000
6[90]	6 710	9 740	.79	1.15	23 430	34 000	11 270	16 350
4[±10, ∓10]	103 400	150 000	14.5	21.1	------	-------	158 500	230 000
8[0, +10, 0, -10, -10, 0, +10, 0]	131 500	191 000	13.1	19.0	------	-------	135 700	197 000
13[±40, 9(0), ∓40]	85 400	124 000	9.6	14.0	------	-------	99 900	145 000

Laminate	Flexural modulus		Short-beam interlaminar shear		Miniature Izod impact energy		Coefficient of thermal expansion	
			N/cm^2	psi	cm-N	in.-lb	$\frac{cm/cm}{°C}$	$\frac{in./in.}{°F}$
6[0]	12.1×10^6	17.6×10^6	11 020	16 000	171.8	15.2	0	0
6[90]	.74	1.07	------	------	20.3	1.8	26.1×10^{-6}	14.5×10^{-6}
4[±10, ∓10]	11.6	16.8	------	------	-----	----	---------	---------
8[0, +10, 0, -10, -10, 0, +10, 0]	13.1	19.0	------	------	-----	----	---------	---------
13[±40, 9(0), ∓40]	6.4	9.3	------	------	-----	----	---------	---------

TABLE III. - ELASTIC AND THERMAL PROPERTIES OF HT-S FIBER AND PMR-PI MATRIX CONSTITUENTS USED IN COMPOSITE MICROMECHANICS

[f(m) denotes fiber or matrix property.]

Property	HT-S fiber	PMR-PI matrix
Moduli, N/cm^2; psi		
$E_{f(m)11}$	26.2×10^6; 38.0×10^6	0.32×10^6; 0.47×10^6
$E_{f(m)22}$	1.4×10^6; 2.0×10^6	0.32×10^6; 0.47×10^6
$G_{f(m)12}$	1.7×10^6; 2.5×10^6	0.12×10^6; 0.17×10^6
Poisson's ratio, $\nu_{f(m)12}$	0.25; 0.25	0.36; 0.36
Thermal coefficients of expansion, cm/cm/^{o}C; in./in./^{o}F:		
$\alpha_{f(m)11}$	-0.018×10^{-6}; 0.01×10^{-6}	50.4×10^{-6}; 28.0×10^{-6}
$\alpha_{f(m)22}$	10.1×10^{-6}; 5.6×10^{-6}	50.4×10^{-6}; 28.0×10^{-6}
Heat conductivities, J/m-sec-^{o}C; $(Btu/ft^2)/^{o}F/in.$:		
$K_{f(m)11}$	1.09×10^9; 580	2.35×10^6; [a]1.25
$K_{f(m)22}$	1.09×10^8; 58	2.35×10^6; [a]1.25
$K_{f(m)33}$	1.09×10^8; 58	2.35×10^6; [a]1.25
Weight density, $\rho_{f(m)}$, g/cm^3; $lb/in.^3$	1.8; 0.065	1.2; 0.044

[a]Estimated.

TABLE IV. - CONSTITUENT PROPERTIES FOR MICROMECHANICS STRENGTH PREDICTIONS

Fiber tensile strength, S_{fT}, N/cm^2; ksi	242×10^3; 350
Matrix compressive strength, S_{mC}, N/cm^2; psi	11.3×10^3; 16.5
Matrix tensile strain, ϵ_{mpT}, cm/cm; in./in.	0.018; 0.018
Matrix compressive strain, ϵ_{mpC}, cm/cm; in./in.	0.035; 0.035
Matrix shear strain, ϵ_{mpS}, cm/cm; in./in.	0.050; 0.050
Matrix torsional strain, ϵ_{mpTOR}, cm/cm; in./in.	0.050; 0.050

TABLE V. - MICROMECHANICS STRENGTH

CORRELATION COEFFICIENTS

Longitudinal tensile strength:	
β_{fT}	0.94
β_{mT}	1.00
Longitudinal compressive strength:	
Matrix compression limited -	
β_{fC}	0.17
β_{mC}	1.00
Intralaminar shear limited -	
a_1	13.30
a_2	31 900
Transverse tensile strength:	
β_{22T}	1.06
β_{22C}	1.60
Intralaminar shear strength, β_{12S}	1.00
Delamination, β_{DEL}	16.5

TABLE VI. - HT-S/PMR-PI MEASURED AND PREDICTED UNIDIRECTIONAL COMPOSITE MECHANICAL PROPERTIES FOR A 55 VOLUME PERCENT FIBER CONTENT COMPOSITE

Property	Measured	Predicted
Moduli, N/cm^2; psi:		
Longitudinal, $E_{\ell 11}$	15.0×10^6; 21.7×10^6	14.5×10^6; 21.1×10^6
Transverse, $E_{\ell 22}$	0.83×10^6; 1.2×10^6	0.83×10^6; 1.2×10^6
Shear, $G_{\ell 12}$	----------	0.50×10^6; 0.72×10^6
Poisson's ratio, $\nu_{\ell 12}$	----------	0.24
Thermal coefficient of expansion, cm/cm/°C; in./in./°F:		
Longitudinal, $\alpha_{\ell 11}$	~0	0.49×10^{-6}; 0.27×10^{-6}
Transverse, $\alpha_{\ell 22}$	25.6×10^{-6}; 14.2×10^{-6}	26.1×10^{-6}; 14.5×10^{-6}
Thermal heat conductivity, J/m-sec-°C; (Btu/hr)/ft^2/°F/in.:		
Longitudinal, $K_{\ell 11}$	----------	6.02×10^8; 320
Transverse, $K_{\ell 22}$	----------	8.27×10^6; 4.4
Through-the-thickness, $K_{\ell 33}$	----------	8.27×10^6; 4.4
Strengths, N/cm^2; ksi:		
Longitudinal tensile, $S_{\ell 11T}$	125×10^3; 182	126×10^3; 183
Longitudinal compressive, $S_{\ell 11C}$	94×10^3; 136	95×10^3; 138
Transverse tensile, $S_{\ell 22T}$	6.6×10^3; 9.6	6.2×10^3; 9.0
Transverse compressive, $S_{\ell 22C}$	[a] 23.4×10^3; 34.0	[c] 18.0×10^3; 26.1
Intralaminar shear, $S_{\ell 12S}$	[b] 11.0×10^3; 16.0	[d] 5.5×10^3; 8.0
Coefficient for combines stress	----------	1.09

[a] Maximum value with considerable nonlinearity.

[b] Short-beam-shear stress.

[c] About 80 percent of maximum value was used.

[d] One-half of short-beam-shear stress was used.

TABLE VII. - LAMINATE ELASTIC CONSTANTS AND THERMAL COEFFICIENTS OF EXPANSION

[HT-S/PMR-PI; fiber content, 55 vol %; weight density, 1.6 g/cm^3 (0.056 lb/in.^{3}).]

Laminate	Modulus						Poisson's ratio, ν_{cxy}	Thermal coefficients of expansion			
	E_{cxx}		E_{cyy}		G_{cxy}			α_{cxx}		α_{cyy}	
	N/cm^2	psi	N/cm^2	psi	N/cm^2	psi		cm/cm/$^\circ$C	in./in./$^\circ$F	cm/cm/$^\circ$C	in./in./$^\circ$F
6[0]	14.5×10^6	21.1×10^6	0.83×10^6	1.20×10^6	0.50×10^6	0.72×10^6	0.24	0.49×10^{-6}	0.27×10^{-6}	26.1×10^{-6}	14.5×10^{-6}
4[+10, -10, -10, +10]	13.4	19.4	.83	1.20	.90	1.30	.68	-.11	-.06	25.0	13.9
8[0, +10, 0, -10, -10, 0, +10, 0]	14.0	21.3	.83	1.20	.69	1.00	.46	.02	.01	25.6	14.2
13[+40, -40, 9(0), -40, +40]	11.0	16.0	1.52	2.20	1.45	2.10	.73	-.13	-.07	13.0	7.2
4[+40, -40, -40, +40]	2.3	3.4	1.40	2.00	3.65	5.30	1.00	-.70	-.39	6.03	3.35

TABLE VIII. - LAMINATE 13[±40, 9(0), ∓40] AXIAL AND BENDING STIFFNESSES

[HT-S/PMR-PI; fiber content, 55 vol %; weight density, 1.6 g/cm^3 (0.056 lb/in.^{3}).]

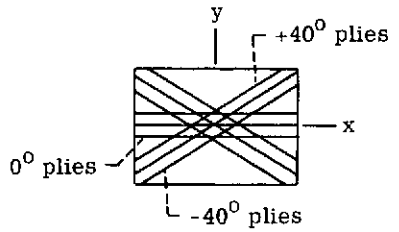

Ply orientation schematic

Plate bending stiffnesses	Value	
	cm-N	in.-lb
Bending along x, D_{c11}	14 377	1272
Bending along y, D_{c22}	4 160	368
Coupled bending x with y, D_{c12}	3 832	339
Coupled x-bending with twisting, D_{c13}	780	69
Coupled y-bending with twisting, D_{c23}	565	50
Twisting, D_{c33}	4 318	382

TABLE IX. - PLY STRESSES IN LAMINATE 6(0)

[HT-S/PMR-PI; fiber content, 55 vol %.]

Ply	Thermal load due to cure[a]				Mechanical load				Combined loads			
	$\sigma_{\ell 11}$	$\sigma_{\ell 22}$	$\sigma_{\ell 12}$	Margin of safety	$\sigma_{\ell 11}$	$\sigma_{\ell 22}$	$\sigma_{\ell 12}$	Margin of safety	$\sigma_{\ell 11}$	$\sigma_{\ell 22}$	$\sigma_{\ell 12}$	Margin of safety
	N/cm^2 (ksi)				N/cm^2 (ksi)				N/cm^2 (ksi)			
Axial force, 42 200 N (9500 lb)												
All	0 (0)	0 (0)	0 (0)	1.00	128×10^3 (186)	0 (0)	0 (0)	-0.04	128×10^3 (186)	0 (0)	0 (0)	-0.04
Bending moment, 1030 cm-N (91 in.-lb)												
Bottom	0 (0)	0 (0)	0 (0)	1.0	121×10^3 (175)	0 (0)	0 (0)	0.09	121×10^3 (175)	0 (0)	0 (0)	0.09
Top	0 (0)	0 (0)	0 (0)	1.0	-121 (-175)	0 (0)	0 (0)	-1.20	-121 (-175)	0 (0)	0 (0)	-1.20

[a] ΔT = -294 C° (-530 F°).

TABLE X. - PLY STRESSES IN LAMINATE 4(±10, ∓10)

[HT-S/PMR-PI; fiber content, 55 vol %.]

Ply	Thermal load due to cure[a]				Mechanical load				Combined loads			
	$\sigma_{\ell 11}$	$\sigma_{\ell 22}$	$\sigma_{\ell 12}$	Margin of safety	$\sigma_{\ell 11}$	$\sigma_{\ell 22}$	$\sigma_{\ell 12}$	Margin of safety	$\sigma_{\ell 11}$	$\sigma_{\ell 22}$	$\sigma_{\ell 12}$	Margin of safety
	N/cm^2 (ksi)				N/cm^2 (ksi)				N/cm^2 (ksi)			
Axial force, 24 910 N (5600 lb)												
+10	-0.5×10^3 (-0.7)	0.5×10^3 (0.7)	-1.2×10^3 (-1.8)	0.94	104×10^3 (151)	-2.5×10^3 (-3.6)	-2.1×10^3 (-3.1)	0.04	103×10^3 (150)	-2.0×10^3 (-2.9)	-3.4×10^3 (-4.9)	-1.57
-10	-.5 (-.7)	.5 (.7)	1.2 (1.8)	.94	104 (151)	-2.5 (-3.6)	2.1 (3.1)	.04	103 (150)	-2.0 (-2.9)	3.4 (4.9)	-1.57
Bending moment, 622 cm-N (55 in. -lb)												
Bottom +10	-0.5×10^3 (-0.7)	-0.5×10^3 (-0.7)	-1.2×10^3 (-1.8)	0.94	104×10^3 (153)	0.5×10^3 (0.7)	-12.6×10^3 (-18.3)	-4.98	105×10^3 (153)	0.9×10^3 (1.3)	-13.8×10^3 (-20.1)	-6.07
Top +10	-.5 (-.7)	-.5 (-.7)	-1.2 (-1.8)	.94	-104 (-153)	-.5 (-.7)	12.6 (18.3)	-5.98	-106 (-154)	~0 (~0)	11.4 (16.5)	-5.01

[a] ΔT = -294 C^o (-530 F^o).

TABLE XI. - PLY STRESSES IN LAMINATE 8[0, +10, 0, -10, -10, 0, +10, 0]

[HT-S/PMR-PI, fiber content, 55 vol %.]

Ply	Thermal load due to cure[a]				Mechanical load				Combined load			
	$\sigma_{\ell 11}$	$\sigma_{\ell 22}$	$\sigma_{\ell 12}$	Margin of safety	$\sigma_{\ell 11}$	$\sigma_{\ell 22}$	$\sigma_{\ell 12}$	Margin of safety	$\sigma_{\ell 11}$	$\sigma_{\ell 22}$	$\sigma_{\ell 12}$	Margin of safety
	N/cm^2 (ksi)				N/cm^2 (ksi)				N/cm^2 (ksi)			
Axial force, 63 500 N (14 270 lb)												
0	1.4×10^3 (2.0)	0.1×10^3 (0.2)	~0 (~0)	1.00	135×10^3 (196)	-1.7×10^3 (-2.5)	~0 (~0)	-0.31	136×10^3 (198)	-1.5×10^3 (-2.2)	~0 (~0)	-0.26
+10	-1.9 (-2.7)	.3 (.5)	-1.2×10^3 (-1.8)	.94	130 (188)	-1.4 (-2.1)	-2.3×10^3 (-3.4)	-.31	128 (185)	-1.1 (-1.6)	-3.6×10^3 (-5.2)	-.51
-10	-1.9 (-2.7)	.3 (.5)	1.2 (1.8)	.94	130 (188)	-1.4 (-2.1)	2.3 (3.4)	-.31	128 (185)	-1.1 (-1.6)	3.6 (5.2)	-.51
Bending moment, 2113 cm-N (187 in.-lb)												
Bottom												
0	1.4×10^3 (2.0)	0.1×10^3 (0.2)	~0 (~0)	1.00	128×10^3 (185)	-0.7×10^3 (-1.0)	-4.3×10^3 (-6.3)	-0.68	129×10^3 (187)	-0.5×10^3 (-0.7)	-4.3×10^3 (-6.3)	-0.69
+10	-1.9 (-2.7)	.3 (.5)	-1.2×10^3 (-1.8)	.94	72 (104)	.3 (.5)	-4.3 (-6.3)	.64	70 (102)	.6 (.9)	-5.6 (-8.1)	-.33
Top												
0	1.4 (2.0)	.1 (.2)	~0 (~0)	1.00	-128 (-185)	.7 (1.0)	4.3 (6.3)	-2.23	-126 (-183)	.9 (1.3)	4.3 (6.3)	-2.22
+10	-1.9 (-2.7)	.3 (.5)	-1.2 (-1.8)	.94	-72 (-104)	.3 (.5)	4.3 (6.3)	-.40	-74 (-107)	~0 (~0)	3.0 (4.4)	-.14

[a] ΔT = -294.5 C^o (-530 F^o).

TABLE XII. - PLY STRESSES IN LAMINATE 13[+40, -40, 9(0), -40, +40]

[HT-S/PMR-PI; fiber content, 55 vol %.]

Ply	Thermal load due to cure[a]				Mechanical load				Combined loads			
	$\sigma_{\ell 11}$	$\sigma_{\ell 22}$	$\sigma_{\ell 12}$	Margin of safety	$\sigma_{\ell 11}$	$\sigma_{\ell 22}$	$\sigma_{\ell 12}$	Margin of safety	$\sigma_{\ell 11}$	$\sigma_{\ell 22}$	$\sigma_{\ell 12}$	Margin of safety
	N/cm^2 (ksi)				N/cm^2 (ksi)				N/cm^2 (ksi)			
Axial force, 57 840 N (13 000 lb)												
+40	-19.4×10^3 (-28.1)	4.3×10^3 (6.2)	-1.9×10^3 (-2.7)	0.21	31.7×10^3 (46.0)	0.3×10^3 (0.5)	-6.4×10^3 (-9.3)	-0.44	12.3×10^3 (17.9)	4.6×10^3 (6.7)	-8.3×10^3 (-12.1)	-1.80
-40	-19.4 (-28.1)	4.3 (6.2)	1.9 (2.7)	.21	31.7 (46.0)	.3 (.5)	6.4 (9.3)	-.44	12.3 (17.9)	4.6 (6.7)	8.3 (12.1)	-1.80
0	3.4 (5.0)	3.2 (4.7)	~0 (~0)	.74	110.2 (160.0)	-3.1 (-4.5)	~0 (~0)	.07	113.7 (165)	.2 (.3)	~0 (~0)	.20
Bending moment, 1854 cm-N (164 in.-lb)												
Bottom												
+40	-19.4×10^3 (-28.1)	4.3×10^3 (6.2)	-1.9×10^3 (-2.7)	0.21	21.9×10^3 (31.8)	-0.3×10^3 (-0.5)	7.8×10^3 (11.4)	-1.11	2.6×10^3 (3.7)	3.9×10^3 (5.7)	-9.8×10^3 (-14.2)	-2.57
-40	-19.4 (-28.1)	4.3 (6.2)	1.9 (2.7)	.21	25.4 (35.5)	-.6 (-.8)	6.5 (9.4)	-.46	5.2 (7.5)	3.7 (5.4)	8.3 (12.1)	-1.67
0	3.4 (5.0)	3.2 (4.7)	~0 (~0)	.74	80.6 (117)	-3.1 (-4.5)	-.2 (-.3)	.45	84.1 (122)	.1 (.2)	-.1 (-.2)	.56
Top												
+40	-19.4 (-28.1)	4.3 (6.2)	-1.9 (-2.7)	.21	-21.9 (-31.8)	.3 (.5)	7.8 (11.4)	-1.17	-41.2 (-59.8)	4.5 (6.6)	6.0 (8.7)	-1.36
-40	-19.4 (-28.1)	4.3 (6.2)	1.9 (2.7)	.21	25.4 (35.5)	.6 (.8)	-6.5 (-9.4)	-.53	-43.8 (-63.6)	4.8 (7.0)	-4.6 (-6.7)	-.99
0	3.4 (5.0)	3.2 (4.7)	~0 (~0)	.74	-80.6 (-117)	3.1 (4.5)	.2 (.3)	-.68	-77.2 (-112)	6.3 (9.2)	.2 (.3)	-1.86

[a] $\Delta T = -294.5\ C^o$ (-530 F^o).

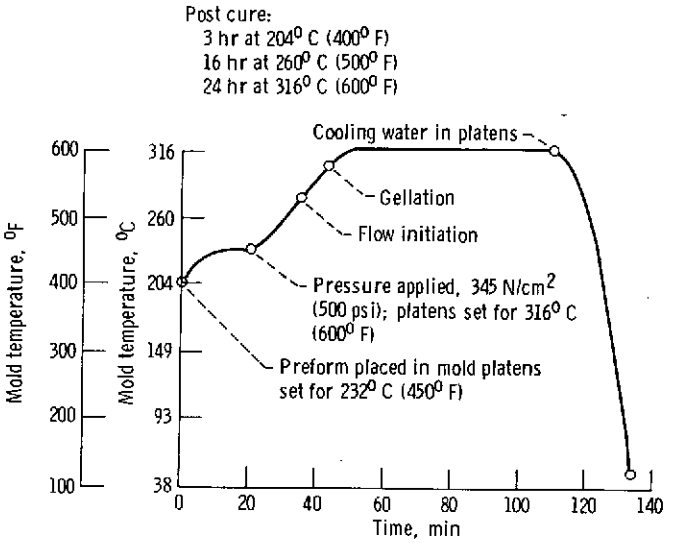

Figure 1. - Molding cycle for PMR-PI laminate.

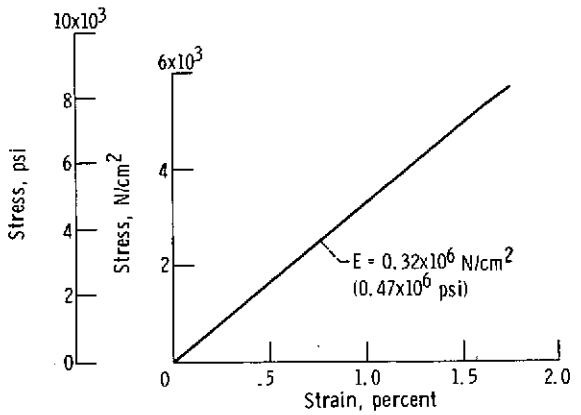

Figure 2. - Stress-strain diagram of PMR-PI neat resin at room temperature.

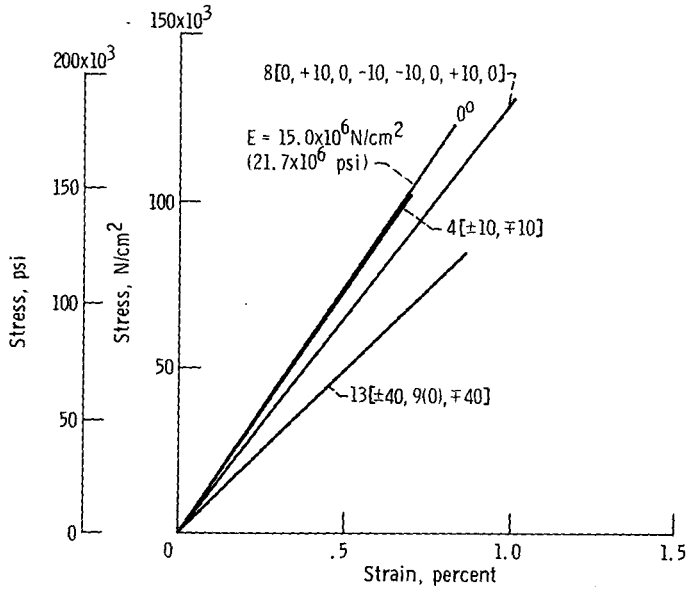

Figure 3. - Stress-strain diagram of various HT-S/PMR-PI angleplied laminates at room temperature.